J Mater Sci (2011) 46:6007–6017
DOI 10.1007/s10853-011-5563-z

Modeling ductile to brittle transition temperature of functionally graded steels by fuzzy logic

Ali Nazari · Amir Ali Milani

Received: 12 January 2011 / Accepted: 23 February 2011 / Published online: 26 April 2011

Abstract In this article, a model based on fuzzy logic (FL) for predicting ductile to brittle transition temperature of functionally graded steels in both crack divider and crack arrester configurations has been presented. Functionally graded steels containing graded ferritic and austenitic regions together with bainite and martensite intermediate layers were produced by electroslag remelting. For purpose of building the model, training and testing using experimental results from 140 specimens produced from two basic composites were conducted. The used data as inputs in FL models are arranged in a format of six input parameters that cover the FGS type, the crack tip configuration, the thickness of graded ferritic region, the thickness of graded austenitic region, the distance of the notch from bainite or martensite intermediate layer, and temperature. According to these input parameters, in the FL, the ductile to brittle transition temperature of each FGS specimen was predicted. It has been found that FL model will be valid within the ranges of variables. The training and testing results in the FL model have shown a strong potential for predicting the ductile to brittle transition temperature of each FGS specimen.

Introduction

Evaluations on damage of the composite and functionally graded structures is of very interesting fields in mechanics of materials [1, 2]. The ductile to brittle transition temperature (DBTT) is a phenomenon which is widely observed in BCC metals and in covalently based materials. Below a critical temperature (DBTT), the materials suddenly lose their ductility. The controlling mechanism of this transition still remains unclear despite of large efforts made in experimental and theoretical investigation. Charpy (CVN) impact test is a widely used test on notched specimens which are submitted to the impact of a hammer with the given kinetic energy [3] to evaluate DBTT. Steel alloys have been investigated extensively during the past years due to its wide application in engineering. Ductile crack growth initiated by the formation of disconnected ductile microcracks can be found in most of steel alloys. However, the mechanism of the formation of microvoids and their special distribution ahead of the crack tip may be different. Recently, Ebrahimi and Seo [4] have investigated crack initiations in a two specific type of steels: a ferritic–pearlitic and a bainitic structural steel. In the ferritic–pearlitic steel, relatively large inclusions, mainly manganese sulfide, were found to be close to the crack tip, where microvoids may form due to high shear stresses, ductile cracks usually grow along the position of these particles. For bainitic steels, geometrical inhomogeneities were found to be the main reason for the formation of local microcracks.

Very few fracture experiments, particularly dynamic fracture, of FGMs have been reported. Among them, crack tip deformation and fracture parameter history in functionally graded glass-filled epoxy were evaluated for low velocity impact loading by Rousseau and Tippur [5]. Guo and Noda [6] studied the dynamic response of a functionally graded layered structure with a crack crossing the interface with in-plane impact loading condition. Xu et al. [7] investigated the plane strain problem of semi-infinite cracks in an infinite functionally graded orthotropic material with opening and in-plane shear impact loading modes.

A. Nazari (✉) · A. A. Milani
Department of Materials Science and Engineering,
Saveh Branch, Islamic Azad University, Saveh, Iran
e-mail: alinazari84@aut.ac.ir

Bezensek and Hancock [8] studied the toughness of laser welded joints of low alloy steel under mode I and mixed mode configuration along with Charpy impact tests.

Functionally graded steels have been produced by electroslag remelting process (ESR) [9]. Studies on transformation characteristics of FGSs produced from austenitic stainless steel and plain carbon steel has revealed that as chromium, nickel, and carbon atoms diffuse at remelting stage, alternating regions with different transformation characteristics are created. When appropriate arrangement and thickness of original ferritic ($\dot{\alpha}$) and original austenitic ($\dot{\gamma}$) steels is selected to make electrodes, composites with graded ferrite, and austenite regions together with bainite or martensite layers may be made as follows [9];

$$(\dot{\alpha}\dot{\gamma})_{\mathrm{el}} \xrightarrow{\mathrm{R}} (\alpha\beta\gamma)_{\mathrm{com}}$$

$$(\dot{\gamma}\dot{\alpha}\dot{\gamma})_{\mathrm{el}} \xrightarrow{\mathrm{R}} (\gamma\mathrm{M}\gamma)_{\mathrm{com}}$$

where α and$\gamma$are graded ferrite and austenite regions in the final composite, respectively, β and M are bainite and martensite layers in the final composite, respectively, el is electrode, com is composite, and R is remelting.

Transformation characteristics [9], tensile strength [10], Charpy impact energy [11–13], and fracture toughness [14, 15] of FGSs has been modeled previously. Since functionally graded steels are made of different structures, investigations on DBTT seem interesting. One may anticipate that by dislocating the crack in graded regions, the transition temperature may be altered. Thus, in this study is to investigate DBTT of FGSs in crack divider configuration (Fig. 1a) together with DBTT of FGSs in crack arrester configuration (Fig. 1b) and different notch tip positions with respect to the bainite or martensite layers.

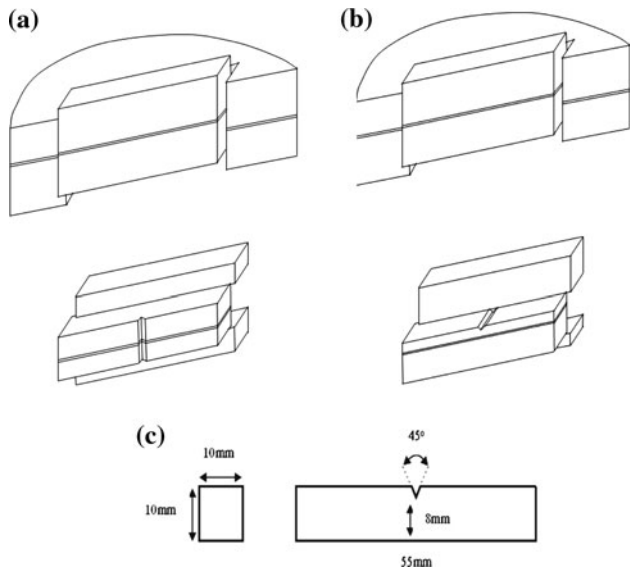

Fig. 1 Schematic representation of Charpy impact specimens' preparation in **a** crack divider, **b** crack arrester configurations, and **c** dimensions of Charpy impact specimen

Over the last two decades, a different modeling method based on fuzzy logic (FL) has become popular and has been used by many researchers for a variety of engineering applications. Fuzzy control theory can be applied on linear and nonlinear systems. It does not need to handle the tedious mathematical models of controlled body. It needs only to set a simple controlling method based on engineering experience. Therefore, it is particularly useful in complicated structural control system. The Charpy impact energy (CVN) can be calculated using the models built with FL. It is convenient and easy to use these models for numerical experiments to review the effects of each variable on the CVN values [16, 17].

The aim of this study is to predict ductile to brittle transition temperature of functionally graded steels in both crack divider and crack arrester configurations by FL. Totally 140 data of Charpy impact tests in different temperatures were collected, trained, and tested by means of FL. The obtained results have been compared by experimental ones to evaluate the software power for predicting the DBTT of FGSs.

Experimental procedure

Similar to the previous studies [9–15], to make FGSs, a miniature ESR apparatus was used. The slag was a mixture of 20% CaO, 20% Al_2O_3, and 60% CaF_2. The original ferritic and austenitic steels which used as electrodes were commercial type AISI 1020 and AISI 316 steels with the chemical composition presented in Table 1.

Two arrangements of ferritic–pearlitic and austenitic steel slices in the form of a two-piece $\dot{\alpha}\dot{\gamma}$ electrode and three-piece $\dot{\gamma}\dot{\alpha}\dot{\gamma}$ electrode were spot welded. The height of each slice in the two-piece $\dot{\alpha}\dot{\gamma}$ electrode was 150 mm and in the three-piece $\dot{\gamma}\dot{\alpha}\dot{\gamma}$ electrode, the height of the middle slice was 25 mm and that of the neighboring slices was 137.5 mm.

Remelting was carried out under a constant power supply of 16KVA. After remelting, composite ingots were hot-pressed at 980 °C down to the thickness of 20 mm, and then were air-cooled.

Table 1 Chemical composition of original ferritic and austenitic steels

	%C	%Si	%Mn	%P	%S	%Cr	%Ni
Original austenite	0.07	1	2	0.045	0.03	18.15	9.11
Original ferrite	0.2	0.3	0.2	0.05	0.05	–	–

The impact energy of FGSs in both crack divider and crack arrester configurations was evaluated by Charpy impact test in the range of 123–573 K, at intervals of 50 K, using standard sized specimens (10 × 10 × 50 mm) according to the ASTM E23 [18]. The dimension of the specimens is shown in Fig. 1c. In crack divider configuration, from the middle of each hot-pressed specimen eight series of Charpy impact specimen was prepared. For crack arrester configuration, from the produced $\alpha\beta\gamma$ composite ingots, and at a certain temperature, eight series of Charpy specimens were produced in some manner that the bainite intermediate layers was placed at different positions with respect to the notch tip; in four series of the specimens the notch was placed in α and in the other four in γ region. The Charpy impact energy test was carried out triplicately and the average of the obtained results was reported. From $\gamma M\gamma$ composite ingots, due to their symmetric configuration, only four series of Charpy impact specimens with different positions of bainite or martensite layers were produced for each certain temperature.

Charpy impact energy of as-received ferritic and austenitic steels which were annealed at 980 °C and then were air-cooled and Charpy impact energy of single-phase bainite and martensite with composition and mechanical properties analogous to the bainite and martensite layers was also measured in the range of 123–573 K, at intervals of 50 K. The production method of single-phase specimens with chemical composition and mechanical properties identical to the bainitic and martensitic layers was similar to the previous works [11, 12]. To do this, Charpy impact specimens of the same composition and mechanical properties to bainitic and martensitic layers were produced. Initially, the average chemical composition of bainite and martensite layers was obtained (Table 2). Afterward, bainitic and martensitic samples with the chemical composition in accordance to the average chemical composition of bainitic and martensitic layers were produced by means of a vacuum induction furnace. Similar to the primary composites, the hot-pressing process was carried out at 980 °C, followed by air cooling. Through trial and error (i.e., conforming the chemical composition and changing the cooling rate), the samples with the nearest hardness to bainitic and martensitic layers were selected and Charpy impact test specimens from the bainitic and martensitic samples were made. Charpy impact test results of single-phase bainite and martensite specimens produced from the sample are shown in Table 3 [11, 12].

For metallographic examinations, the plates were sliced, ground, polished, and etched in a "Kalling" solution and 1 pct "Nital."

Vickers microhardness tests were carried out using 100 g weight to evaluate microhardness profile and to verify the location of bainite or martensite intermediate layers.

Table 2 Chemical composition (wt%) of bainitic and martensitic layers together with the single-phase bainite and martensite specimens produced from samples

Specimen studied	Pct Cr	Pct Ni	Pct C	Pct Si	Pct Mn	Pct S	Pct P
Single-phase bainite	14.5	7.2	0.12	0.8	1.8	0.03	0.04
Bainite specimen produced from the sample	14.7	7.15	0.13	0.85	1.9	0.032	0.045
Single-phase martensite	7.3	3.2	0.19	0.39	0.3	0.04	0.05
Martensite specimen produced from the sample	7.38	3.14	0.21	0.28	0.28	0.033	0.055

Table 3 Impact test results of the original ferrite, original austenite, and single-phase bainite specimen

Temperature (K)	Charpy impact energy (J)			
	Original ferrite ($\dot{\alpha}$)	Original austenite ($\dot{\gamma}$)	Bainite specimen produced from the sample	Martensite specimen produced from the sample
123	22	135	95	8
173	30	136	102	8
223	42	138	104	9
273	60	139	106	10
323	68	142	110	11
373	74	146	113	11
423	80	148	115	11
473	88	149	119	12
523	92	151	123	12
573	96	154	127	13

Experimental results

Figure 2a and b illustrate Vickers microhardness profile of $\alpha\beta\gamma$ and $\gamma M\gamma$ composites. The thickness of martensite layer is 1.5 mm and that of bainite is 0.6 mm, which was verified by Vickers microhardness examination and is in accordance to the previous studies [9–15]. In addition, Fig. 3 shows the formation of bainite and martensite layers in the produced composites.

DBTT of the specimens in crack divider configuration

Figure 4 shows that the Charpy impact energy of $\alpha\beta\gamma$ specimens is strongly depended on the containing phases and the temperature of the examination. When the specimen is examined at temperatures more than the room conditions, the Charpy impact energy of $\alpha\beta\gamma$ composites is between that of ferritic–pearlitic steel and austenitic steel (Table 3). On the other hand, when the specimens are tested at low temperatures, a relatively large loss in energy is observed. Once again, the Charpy impact energy of $\alpha\beta\gamma$ composites is between that of ferritic–pearlitic steel and austenitic steel. This condition is similar to the previous studies [11, 12]. A DBTT was found equal to 252 K by data fitting for $\alpha\beta\gamma$ composite in crack divider configuration (Table 4).

Figure 4 shows that in $\gamma M\gamma$ composite no DBTT is appeared. Since martensite layer has a brittle behavior in all temperatures, it controls the fracture energy of the specimen and relatively low impact energy is observed for this specimen. The controlling mechanism of martensite layer has been fully discussed in the previous studies [11, 12].

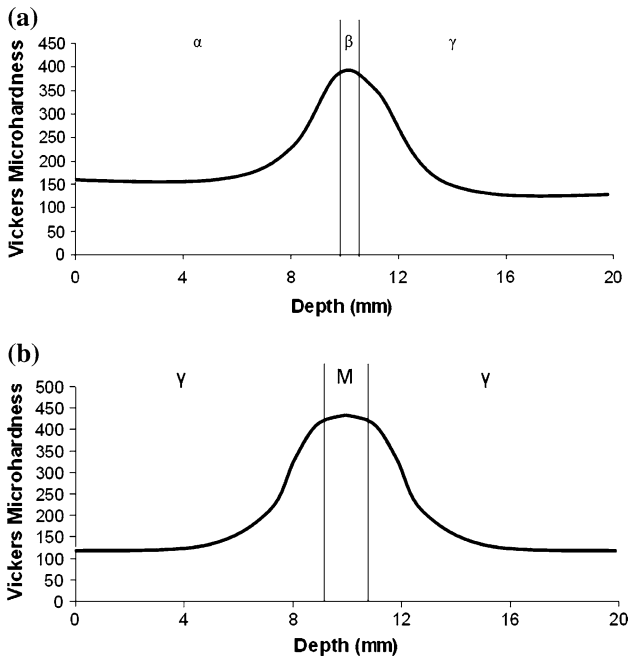

Fig. 2 Microhardness profile of the hot-pressed **a** $\alpha\beta\gamma$ and **b** $\gamma M\gamma$ composite ingots

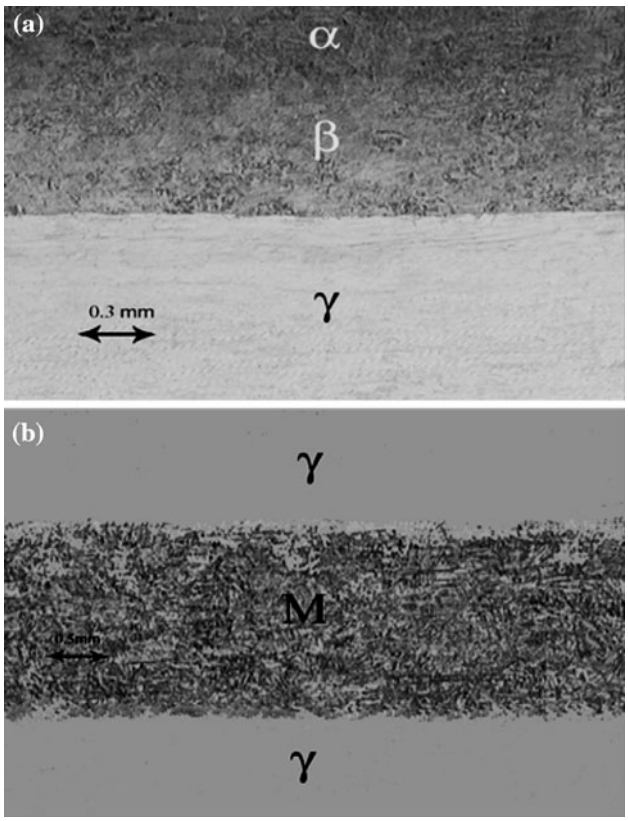

Fig. 3 Microstructure of **a** bainite layer formed in $\alpha\beta\gamma$ composite and **b** martensite layer formed between two layers of austenitic region in $\gamma M\gamma$ composite

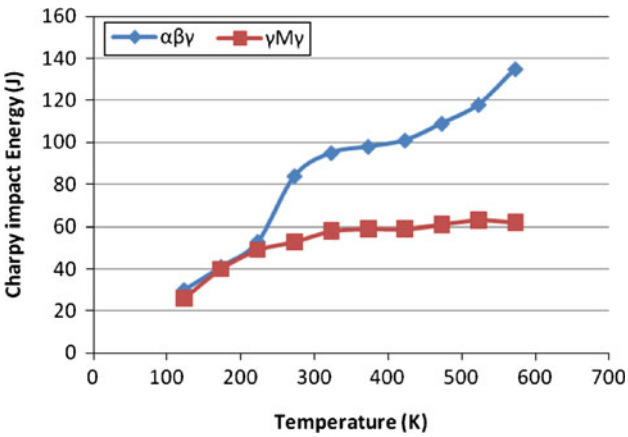

Fig. 4 Variations of Charpy impact energy of $\alpha\beta\gamma$ and $\gamma M\gamma$ composites in crack divider configuration

DBTT of the specimens in crack arrester configuration

DBTT for the specimens was obtained by fitting a 3-order polynomial function on each curve and equating the second

Table 4 Experimental and predicted CVN values by FL models for FGS specimens

Sample designation	Crack tip configuration	The distance of the notch from β or M layers	DBTT values (K)	
			Experimental	Predicted by FL model
$\alpha\beta\gamma$	Divider	–	252	249
$\alpha\beta\gamma$ (Notch in α)	Arrester	1	238	231
$\alpha\beta\gamma$ (Notch in α)	Arrester	2	285	281
$\alpha\beta\gamma$ (Notch in α)	Arrester	3	300	292
$\alpha\beta\gamma$ (Notch in γ)	Arrester	0	206	200

For the other specimens, no DBTT was observed nor predicted by FL models

derivative of the equation to zero. The obtained results from Fig. 5 for $i = 1$, 2, and 3 are 238, 285, and 300 K, respectively (Table 4) which shows that the closer the notches tip to the bainite layer in alpha region, the lower the DBTT. This again confirms that the plastic deformation zone ahead the notch plays a key role in determining the impact energy of the composites. Table 3 shows that the sensitivity of original ferritic–pearlitic specimen to the variations of temperature is more than that of single-phase bainitic specimen. Therefore, one may anticipate that the specimens with the closer notch tip to the bainitic layer in alpha region have lower sensitivity to the temperature variations. As discussed above, when the notch tip is placed at bainite layer interface in alpha region, the main plastic deformation occurs in bainitic and following austenitic layers. Therefore, in this case, DBTT do not

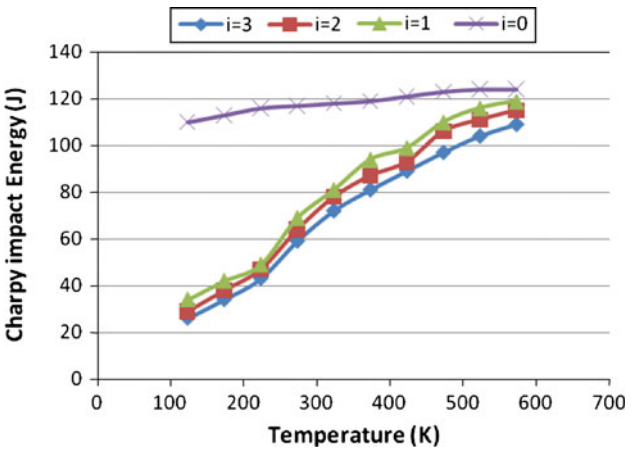

Fig. 5 Variations of Charpy impact energy of $\alpha\beta\gamma$ composites in crack arrester configuration with notch tip located at alpha region by temperature. i denotes the distance of the notch tip with respect to the bainite layer

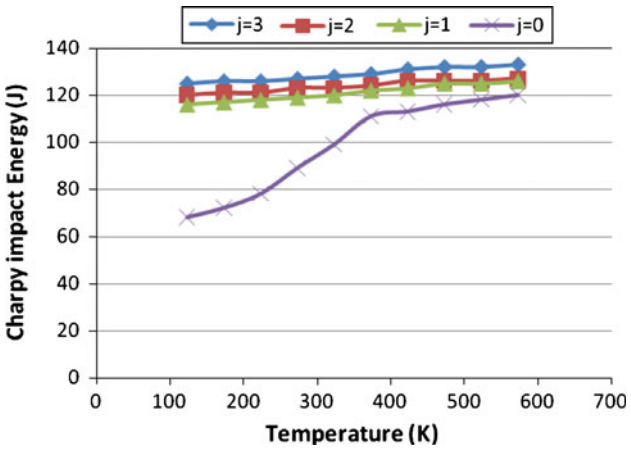

Fig. 6 Variations of Charpy impact energy of $\alpha\beta\gamma$ composites in crack arrester configuration with notch tip located at gamma region by temperature. j denotes the distance of the notch tip with respect to the bainite layer

occur meaningful. In the other words, ductile fracture occurs at every temperature. This is against for the specimens with the notch tip far from the bainite layer which show brittle fracture at low temperatures.

On the other hand, Fig. 6 shows that the Charpy impact energy do not significantly depends on the notch tip position except when the notch is located at the bainite interface. In fact, when the notch tip is far from the bainite layer interface, the plastic deformation occurs in FCC structure of austenitic region which is not sensitive to the temperature variations. Thus, a ductile fracture takes place which prevent showing DBTT. In contrast with alpha region, when the notch tip is located at bainite layer interface at gamma region, the main plastic deformation occurs at bainite layer and following layers of alpha region, thus DBTT (206 K obtained by data fitting) appears.

For $\gamma M\gamma$ composites, no DBTT was observed (Fig. 7). Plastic deformation which occurs in graded FCC gamma region and martensitic layer which are not sensitive to temperature variations may result in constant behavior at all experimental temperatures. When the notch is placed at martensite interface, the ductile fracture occurs since the main part of plastic deformation is in the martensitic layer while a ductile fracture is evident when the notch tip is far from the martensite interface since the plastic deformation takes place in FCC gamma region.

Architecture of FL

Fuzzy set theory was developed by Lotfi Zadeh [19] in 1965 to deal with the imprecision and uncertainty that is often present in realworld applications. In 1974 Mamdani [20], by applying Zadeh's theories of linguistic approach

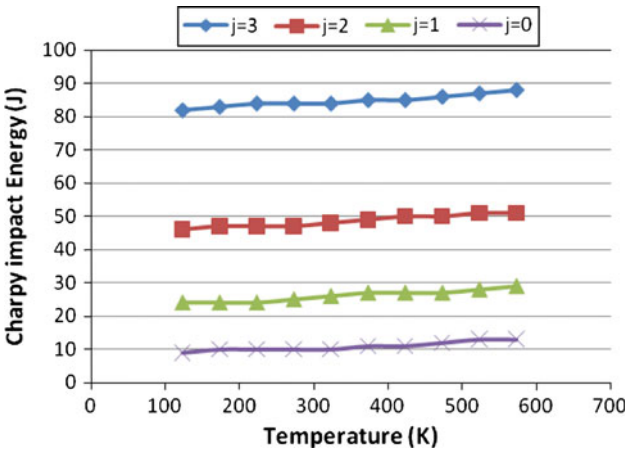

Fig. 7 Variations of Charpy impact energy of $\gamma M\gamma$ composites in crack arrester configuration by temperature. j denotes the distance of the notch tip with respect to the martensite layer

and fuzzy inference, successfully used the 'IF–THEN' rule on the automatic operating control of steam generator. It does not need to handle the tedious mathematical models of controlled body. It needs only to set a simple controlling method based on engineering experience. Therefore, it is particularly useful in complicated structural control system. Since it does not involve complicated mathematical calculations and time of system, delay is reduced in process of operations, lowering its impact on the controlling effects can be expected. Furthermore, since the fuzzy control method is easy to comprehend and to amend, it can be adjusted according to the actual situation. It effectiveness is therefore confirmed. Now, fuzzy control has become most successfully in application of fuzzy theory.

In this part of study, the developed FL-based model was applied to predict the Charpy impact energy data obtained from experiments. The fuzzy rules were written for this purpose. It can be seen from Fig. 8 that we devised the FL-based algorithm model by using the FL toolbox in MATLAB.

The FL model had six input parameters and one output parameters.

The parameters FGS type (F), the crack tip configuration (C), the thickness of graded ferritic region (A), the thickness of graded austenitic region (G), the distance of the notch from bainite or martensite intermediate layer (D), and temperature (T) were set as input variables. The model output variable was the Charpy impact energy (CVN). Membership functions for input and output parameters used for fuzzy modeling are given in Fig. 8. The choice of the membership functions is based on the experiences gained, and their base values are selected so that they are concentrated on more sensitive regions. From the experiments, totally 140 data were achieved and used as target. The input and target values have been given in Table 5. From the total 140 data, 123 data were randomly selected for training set and the other 23 data were used for testing set. The fuzzy rules were written for predict the Charpy impact energy. These rules are obtained as in the following:R_i: (F is F_j) and (C is C_k) and (A is A_m) and (G is G_n) and (D is D_k) and (T is T_n) THEN (CVN is CVN_p) $i = 1,\ldots,2$, $j = 1,\ldots,3$, $k = 1,\ldots,4$, $m = 1,\ldots,5$, $n = 1,\ldots,6$, $p = 1,\ldots,9$.

The assignment of initial related parameters may also influence the performance of the FL to a great extent. However, there is no well defined rule or procedure to have an optimal architecture and parameter settings where the trial and error method still remains valid. This process is very time consuming [21–24]. In this study the MATLAB FL toolbox is used for FL applications. To overcome optimization difficulty, a program has been developed in MATLAB which handles the trial and error process automatically [21–24]. The program tries various numbers of parameters for the algorithm when the highest RMSE (Root Mean Squared Error) of the testing set, as the training of the testing set is achieved [21–24].

Results and discussion

In this study, the error arose during the training and testing in FL model can be expressed as absolute fraction of variance (R^2) which are calculated by Eq. 6 [25]:

$$R^2 = 1 - \left(\frac{\sum_i (t_i - o_i)^2}{\sum_i (o_i)^2} \right) \quad (1)$$

where t is the target value and o is the output value.

All of the results obtained from experimental studies and predicted by using the training and testing results of FL model are given in Fig. 9a and b, respectively. The linear least square fit line, its equation and the R^2 values were shown in these figures for the training and testing data. Also, inputs values and experimental results with testing results obtained from FL model were given in Table 5. As it is visible in Fig. 9, the values obtained from the training and testing in FL model are very close to the experimental results. The result of testing phase in Fig. 9 shows that the FL model is capable of generalizing between input and output variables with reasonably good predictions.

The performance of the FL model is shown in Fig. 9. The best value of R^2 is 99.63% for training set. The minimum value of R^2 is 99.46% for testing set. All R^2 values show that the proposed FL model is suitable and can predict CVN values for every age very close to the experimental values.

From the predicted results, the variations of CVN values versus temperature were obtained and by data fitting the DBTT values derived for each specimen. These values are

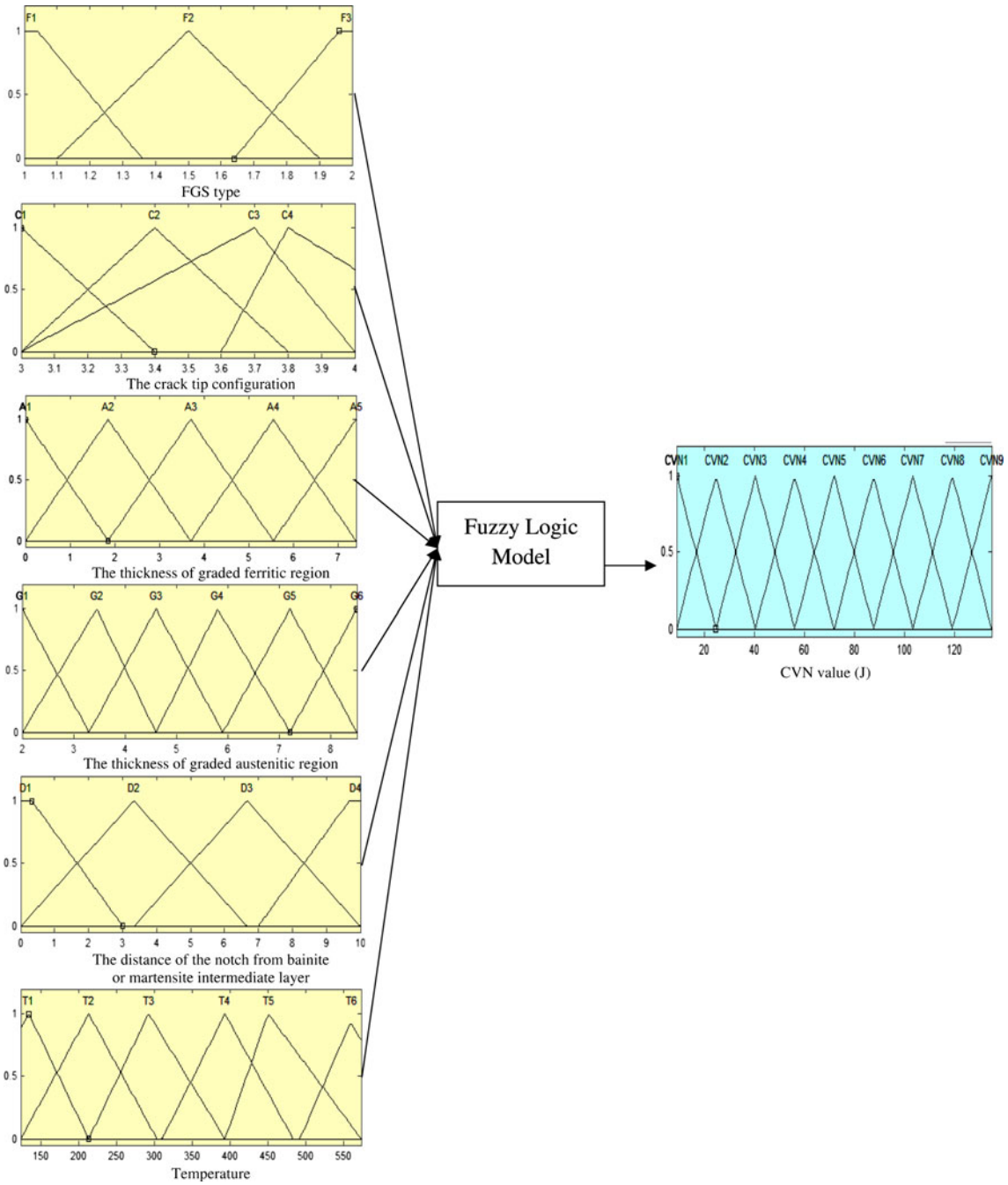

Fig. 8 Block diagram used for fuzzy modeling

listed in Table 4 and as it is observed, there is a meaningful agreement between the experimental and predicted results.

Conclusions

1. In crack divider configuration, DBTT was found for $\alpha\beta\gamma$ composite while no DBTT was observed for $\gamma M\gamma$ composite.
2. In crack arrester configuration, DBTT was evident for the specimens with the notches placed at alpha region of $\alpha\beta\gamma$ composites (except when the notch is placed at bainite interface) and for the specimen with the notch placed at bainite interface in gamma region of $\alpha\beta\gamma$ composite.
3. In crack arrester configuration, DBTT was not occurred for $\gamma M\gamma$ composites, $\alpha\beta\gamma$ composites with the notch placed at bainite interface in alpha region

Table 5 Data sets for comparison of experimental results with results predicted from the FL models

FGS type (F)[a]	The crack tip configuration (C)[b]	The thickness of graded ferritic region (A)	The thickness of graded austenitic region (G)	The distance of the notch from bainite or martensite intermediate layer (D)[c]	Temperature (T)	CVN value obtained from experiments (J)	CVN values predicted by FL model (J)
1	3	5	4.4	10	123	30	29
1	3	5	4.4	10	173	41	33.7
1	3	5	4.4	10	223	53	58.4
1	3	5	4.4	10	273	84	79.9
1	3	5	4.4	10	323	95	94.7
1	3	5	4.4	10	373	98	101.5
1	3	5	4.4	10	423	101	105.1
1	3	5	4.4	10	473	109	111.9
1	3	5	4.4	10	523	118	122.7
1	3	5	4.4	10	573	135	136.1
1	4	2	7.4	0	123	110	110
1	4	2	7.4	0	173	113	111.6
1	4	2	7.4	0	223	116	114.2
1	4	2	7.4	0	273	117	117
1	4	2	7.4	0	323	118	119.5
1	4	2	7.4	0	373	119	121.6
1	4	2	7.4	0	423	121	122.9
1	4	2	7.4	0	473	123	123.5
1	4	2	7.4	0	523	124	123.3
1	4	2	7.4	0	573	124	122.7
1	4	3	6.4	1	123	34	32.7
1	4	3	6.4	1	173	42	42.8
1	4	3	6.4	1	223	49	54.7
1	4	3	6.4	1	273	69	66.9
1	4	3	6.4	1	323	81	78.8
1	4	3	6.4	1	373	94	89.9
1	4	3	6.4	1	423	99	99.9
1	4	3	6.4	1	473	110	108.4
1	4	3	6.4	1	523	116	115.3
1	4	3	6.4	1	573	119	120.9
1	4	4	5.4	2	123	29	29.3
1	4	4	5.4	2	173	38	38.8
1	4	4	5.4	2	223	47	51
1	4	4	5.4	2	273	64	63.9
1	4	4	5.4	2	323	78	76.2
1	4	4	5.4	2	373	87	87.2
1	4	4	5.4	2	423	93	96.4
1	4	4	5.4	2	473	106	104.1
1	4	4	5.4	2	523	111	110.8
1	4	4	5.4	2	573	115	117.9
1	4	5	4.4	3	123	26	37.7
1	4	5	4.4	3	173	34	43.1
1	4	5	4.4	3	223	43	51.4
1	4	5	4.4	3	273	59	60.7
1	4	5	4.4	3	323	72	69.8
1	4	5	4.4	3	373	81	78.5
1	4	5	4.4	3	423	89	87.1

Table 5 continued

FGS type (F)[a]	The crack tip configuration (C)[b]	The thickness of graded ferritic region (A)	The thickness of graded austenitic region (G)	The distance of the notch from bainite or martensite intermediate layer (D)[c]	Temperature (T)	CVN value obtained from experiments (J)	CVN values predicted by FL model (J)
1	4	5	4.4	3	473	97	95.6
1	4	5	4.4	3	523	104	104.2
1	4	5	4.4	3	573	109	112.7
1	4	7.4	2	0	123	68	68.7
1	4	7.4	2	0	173	72	72.1
1	4	7.4	2	0	223	78	80.9
1	4	7.4	2	0	273	89	91.6
1	4	7.4	2	0	323	99	101.5
1	4	7.4	2	0	373	111	11.4
1	4	7.4	2	0	423	113	114.4
1	4	7.4	2	0	473	116	117.6
1	4	7.4	2	0	523	118	119.6
1	4	7.4	2	0	573	120	120.9
1	4	6.4	3	1	123	116	117.4
1	4	6.4	3	1	173	117	114.1
1	4	6.4	3	1	223	118	115
1	4	6.4	3	1	273	119	117.9
1	4	6.4	3	1	323	120	121.1
1	4	6.4	3	1	373	122	123.7
1	4	6.4	3	1	423	123	125.3
1	4	6.4	3	1	473	125	125.8
1	4	6.4	3	1	523	125	125.4
1	4	6.4	3	1	573	126	124.5
1	4	5.4	4	2	123	120	110.5
1	4	5.4	4	2	173	121	117.8
1	4	5.4	4	2	223	121	124
1	4	5.4	4	2	273	123	127.6
1	4	5.4	4	2	323	123	128.6
1	4	5.4	4	2	373	124	127.6
1	4	5.4	4	2	423	126	125.7
1	4	5.4	4	2	473	126	123.8
1	4	5.4	4	2	523	126	122.5
1	4	5.4	4	2	573	127	121.9
1	4	4.4	5	3	123	125	125.5
1	4	4.4	5	3	173	126	123.6
1	4	4.4	5	3	223	126	124.6
1	4	4.4	5	3	273	127	126.4
1	4	4.4	5	3	323	128	127.8
1	4	4.4	5	3	373	129	128.9
1	4	4.4	5	3	423	131	130
1	4	4.4	5	3	473	132	132
1	4	4.4	5	3	523	132	136
1	4	4.4	5	3	573	133	142.9
2	3	0	8.5	10	123	26	44.3
2	3	0	8.5	10	173	40	44.7
2	3	0	8.5	10	223	49	48.4
2	3	0	8.5	10	273	53	54

Table 5 continued

FGS type (F)[a]	The crack tip configuration (C)[b]	The thickness of graded ferritic region (A)	The thickness of graded austenitic region (G)	The distance of the notch from bainite or martensite intermediate layer (D)[c]	Temperature (T)	CVN value obtained from experiments (J)	CVN values predicted by FL model (J)
2	3	0	8.5	10	323	58	59.1
2	3	0	8.5	10	373	59	60.5
2	3	0	8.5	10	423	59	58.8
2	3	0	8.5	10	473	61	59.2
2	3	0	8.5	10	523	63	64.3
2	3	0	8.5	10	573	62	72.1
2	4	0	8.5	0	123	9	11.2
2	4	0	8.5	0	173	10	9.8
2	4	0	8.5	0	223	10	10.3
2	4	0	8.5	0	273	10	10.9
2	4	0	8.5	0	323	10	11.2
2	4	0	8.5	0	373	11	11.4
2	4	0	8.5	0	423	11	11.8
2	4	0	8.5	0	473	12	12.5
2	4	0	8.5	0	523	13	13.5
2	4	0	8.5	0	573	13	14.6
2	4	0	8.5	1	123	24	28.2
2	4	0	8.5	1	173	24	26.2
2	4	0	8.5	1	223	24	26.6
2	4	0	8.5	1	273	25	27.1
2	4	0	8.5	1	323	26	27.1
2	4	0	8.5	1	373	27	26.7
2	4	0	8.5	1	423	27	26.5
2	4	0	8.5	1	473	27	26.8
2	4	0	8.5	1	523	28	27.6
2	4	0	8.5	1	573	29	28.9
2	4	0	8.5	2	123	46	50.5
2	4	0	8.5	2	173	47	48.2
2	4	0	8.5	2	223	47	48.6
2	4	0	8.5	2	273	47	49.5
2	4	0	8.5	2	323	48	49.6
2	4	0	8.5	2	373	49	49.1
2	4	0	8.5	2	423	50	48.8
2	4	0	8.5	2	473	50	49
2	4	0	8.5	2	523	51	49.8
2	4	0	8.5	2	573	51	51.2
2	4	0	8.5	3	123	82	86
2	4	0	8.5	3	173	83	83.8
2	4	0	8.5	3	223	84	84.5
2	4	0	8.5	3	273	84	86
2	4	0	8.5	3	323	84	86.7
2	4	0	8.5	3	373	85	86.6
2	4	0	8.5	3	423	85	86.3
2	4	0	8.5	3	473	86	86.2
2	4	0	8.5	3	523	87	86.8

Table 5 continued

FGS type (F)[a]	The crack tip configuration (C)[b]	The thickness of graded ferritic region (A)	The thickness of graded austenitic region (G)	The distance of the notch from bainite or martensite intermediate layer (D)[c]	Temperature (T)	CVN value obtained from experiments (J)	CVN values predicted by FL model (J)
2	4	0	8.5	3	573	88	87.8

[a] 1 denotes $\alpha\beta\gamma$ and 2 denotes $\gamma M\gamma$ composites

[b] 3 denotes crack divider and 4 denotes crack arrester configurations

[c] 5 is selected for crack divider configuration

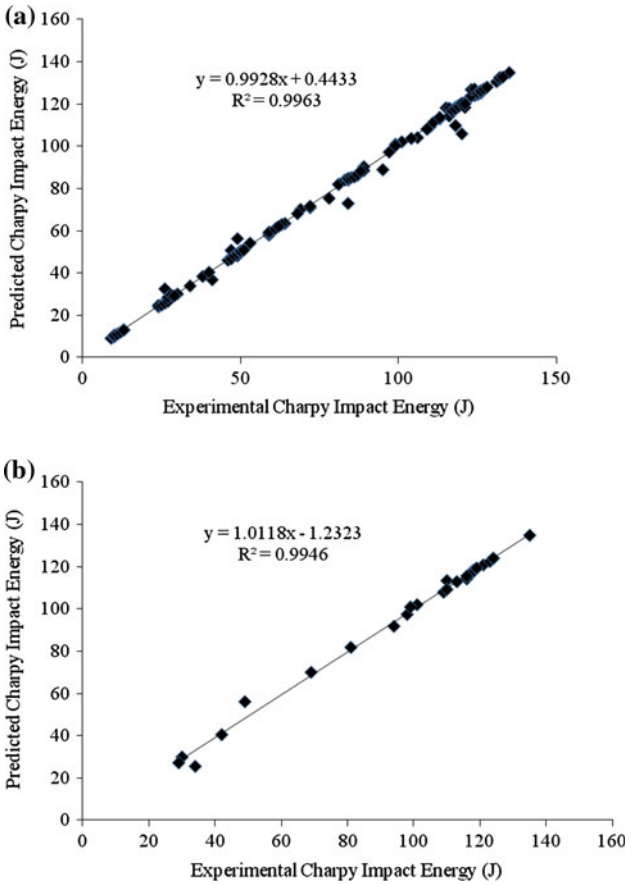

Fig. 9 The correlation of the measured and predicted CVN values in **a** training and **b** testing phase for FL models

and $\alpha\beta\gamma$ composites with the notch placed at gamma region (except when the notch is placed at bainite interface in gamma region).

4. In the whole, in both crack divider and crack arrester configuration, the appearance of DBTT is depended on the containing phases while the fracture behavior of them determines the fracture behavior of the graded specimens.
5. FL can be an alternative approach for the evaluation of the effect of temperature on CVN values and predicting DBTT of FGS specimens. The power of FL model in terms of R^2 showed that FL model is capable to predict suitable results for CVN and DBTT values. However, it has been found that FL model will be valid within the ranges of variables.

References

1. Haj-Ali R (2009) Int J Damage Mech 18(8):691
2. Tay TE, Liu G, Yudhanto A, Tan VBC (2008) Int J Damage Mech 17(1):5
3. Vodopivec F, Arzenšek B, Kmetič D, Vojvodič-Tuma J (2003) MTAEC9 37(6):317
4. Ebrahimi F, Seo HK (1996) Acta Mater 44(2):831
5. Rouseau CE, Tippur HV (2001) Mech Mater 33:403
6. Guo LC, Noda N (2008) Int J Solids Struct 45:336
7. Xu H, Yao X, Feng X, Hisen YY (2008) Mech Mater 40:37
8. Bezensek B, Hancock JW (2007) Eng Fract Mech 74:2395
9. Aghazadeh J-M, Shahosseinie MH (2005) Metall Mater Trans A 36:3471
10. Aghazadeh J-M, Shahosseinie MH, Parastar R-N (2006) Metall Mater Trans A 37:2125
11. Nazari A, Aghazadeh J-M (2010) J Mater Sci Technol 26(11): 1377
12. Nazari A, Aghazadeh J-M (2009) J Mater Sci Technol 25:847
13. Nazari A, Aghazadeh J-M (2010) J Mater Eng Perform 19:1058
14. Aghazadeh Mohandesi J, Nazari A, Hamid Vishkasogheh M, Abedi M (2010) Mater Sci Eng 18:075007
15. Nazari A, Aghazadeh J-M, Riahi SH (2010) Int J Damage Mech. doi: 0.1177/1056789510382851
16. Akkurt S, Tayfur G, Can S (2004) Cement Concr Res 34(8):1429
17. Baykasoğlu A, Dereli T, Tanış S (2004) Cement Concr Res 34(11): 2083
18. ASTM E23 (2001) In: Annual book of ASTM standards, ASTM, Philadelphia
19. Zadeh LA (1965) Inform Control 8:338
20. Mamdani EH (1976) Proc IEEE 121(12):1585
21. Guzelbey IH, Cevik A, Erklig A (2006) J Constr Steel Res 62:962
22. Guzelbey IH, Cevik A, Gögüs MT (2006) J Constr Steel Res 62:950
23. Cevik A, Guzelbey IH (2008) Build Environ 43:751
24. Cevik A, Guzelbey IH (2007) Eng Struct 29(3):383
25. Topcu IB, Sarıdemir M (2008) Comput Mater Sci 41(3):305